doi: 10.17116/engoftalma20151315-1

Optical coherence tomography angiography in the diagnosis of neovascular age-related macular degeneration

T.B. SHAIMOV[1], I.E. PANOVA[1], R.B. SHAIMOV[2], V.A. SHAIMOVA[2], T.A. SHAIMOVA[2], A.V. FOMIN[3]

[1]South-Ural State Medical University, Faculty of Postgraduate Education, Department of Ophthalmology, 64 Vorovskogo St., Chelyabinsk, Russian Federation, 454092; [2]Center "Vision" LLC, 88 Komsomolskiy prospekt, Chelyabinsk, Russian Federation, 454014; [3]Research Institute of Eye Diseases, 11A,B Rossolimo St., Moscow, Russian Federation, 119021

Aim — to determine optical coherence tomography (OCT) angiography signs of classic and occult choroidal neovascularization (CNV) in patients with age-related macular degeneration (AMD) and evaluate their information value in monitoring the effect of anti-VEGF therapy. **Material and methods.** The study enrolled 76 patients (87 eyes), including 68 patients (72 eyes) with wet AMD and 8 patients (15 eyes) with no signs of neovascularization. All patients underwent spectral-domain OCT, OCT angiography, and *fluorescein angiography (*FA). OCT angiography was used to evaluate neovascular networks in terms of their location, shape, size, and extent of visualization. Sensitivity and specificity of the method were assessed separately in a group of 37 CNV eyes and 15 unsuspicious eyes, specific findings at FA being the main diagnostic criteria. To determine the information value of OCT angiography in monitoring the effect of intravitreal ranibizumab therapy, 9 patients (9 eyes) were selected, in whom the exam as performed the day before the injection and then at days 3, 10, 17, 24, and 31. **Results.** The patients were divided into two groups. Group 1 consisted of 43 eyes with occult CNV, group 2 — of 29 eyes with classic CNV. Neovascular loops underneath the retinal pigment epithelium were found in 76.74% of occult CNV cases. In patients with classic CNV, the neovasculature was clearly visible in 82.76% of eyes, loop-like and tree-like networks occurring with similar frequency (51.72% and 42.28% respectively). OCT angiography results obtained prior to and following ranibizumab injection revealed a change in not only the size of neovascularization, but also the density, thickness, and branching pattern of newly formed blood vessels. Sensitivity and specificity of OCT angiography has been shown to be 89.2% and 93.3% respectively. **Conclusion.** OCT angiography enables diagnosis of both classic and occult choroidal neovascularization in patients with AMD as well as dynamic assessment of the size of the neovascular complex during anti-VEGF treatment. The method has high sensitivity and specificity.

Keywords: *optical coherence tomography angiography, OCT angiography, age-related macular degeneration.*

Vestnik_Oftalmologii_2015-5_4EN

The importance of studying age-related macular degeneration (AMD) is determined by its high prevalence among elderly patients, bilateral involvement, and progressive character associated with neovascularization development in 10-20% of cases [1-4]. Neovascular AMD (also, wet AMD), as progresses, causes irreversible vision loss due to central scotoma. In the absence of effective rehabilitation measures, quality of life in end-stage AMD patients decreases [5, 6].

There are two major types of choroidal neovascularization (CNV) identified by D. Gass in 1997. Type 1 CNV is called "occult", implying that new vessels grow beneath the retinal pigment epithelium (RPE), while type 2 CNV, known as "classic", is associated with vessels formation above or at the level of RPE. In clinical practice, one also comes across mixed CNV that can be classified as either "predominantly classic", or "predominantly occult". Moreover, over the past few years, this spectrum has expanded to include atypical forms of CNV such as polypoidal choroidal neovascularization and retinal angiomatous proliferation [7-11].

Standard diagnostic options for neovascular AMD include spectral-domain optical coherence tomography (SD-OCT) and dye tracing methods — fluorescein and indocyanine green angiography (FAG and IAG, respectively). Dye tracing methods suffer from a number of disadvantages, namely invasiveness, the risk of side effects, and two-dimensionality of the acquired images, which complicates localization of the neovascular complex [12-14].

Evolution of optical coherence tomography has led to the development of a brand new diagnostic method in ophthalmology — OCT angiography. Being based on the split-spectrum amplitude decorrelation angiography (SSADA) algorithm [15], OCT angiography enables non-invasive visualization of retinal and choroidal blood flow and gives a clear idea of size, structure, configuration, and location of the newly formed vessels. Since it does not require intravenous dye injection, OCT angiography is free of complications and side effects [15, 16]. It also provides three-dimensional images of the retina and choroid allowing to identify blood flow peculiarities of each of their layers. The high value of information provided by OCT angiography together with its non-invasiveness and the feasibility of frequent follow-ups justify its widespread use in clinical practice.

The aim of this study was to identify distinctive OCT angiography signs of classic and occult CNV in AMD patients and determine their value in monitoring the effect of anti-VEGF therapy.

Material and methods

Clinical and instrumental assessment was performed in 76 patients (87 eyes), of whom 68 (72 eyes) were diagnosed with neovascular AMD. The remaining 8 patients (15 eyes) with drusen-associated RPE detachment, but no signs of neovascularization were enrolled in order to evaluate specificity of OCT angiography.

All patients underwent SD-OCT using RTVue-100 and RTVue XR Avanti (Optovue, USA) machines. The following scan protocols were applied: Line, CrossLine, 3D Macular, 3D Widefield MCT, and AngioRetina. Line and cross line scans were taken with active eye-tracking and averaged by 40-250. Since the AngioRetina protocol of the RTVue XR Avanti OCT utilizes SSADA algorithm, it was applied to perform OCT angiography with scan area size of 2x2, 3x3, and 6x6 mm. All examinations were performed in the macular zone with patient's gaze on central fixation. In case of impaired fixation the patient was re-scanned until clear images with no motion artifacts were obtained.

Fluorescein angiography was performed in 35 patients (37 eyes) on NW8F Plus and TRC-NW7SF Mark II (Topcon, Japan) machines. The contrasting technique was standard, which implies that the patients were injected intravenously with 5 ml of 10% fluorescein (NOVARTIS PHARMA, AG).

En face OCT angiograms were segmented into four layers, namely the superficial vascular plexus, deep vascular plexus, outer retina, and choriocapillaries, using default layer thickness and Z-offset values. In some cases these parameters were adjusted in order to increase image quality.

The following features of neovascular networks were evaluated: size, location, configuration, and extent of visualization. The areas were measured with the Adobe Photoshop CS6 software (Adobe Systems, Inc.).

Sensitivity and specificity of the method were assessed separately in a group of 37 CNV eyes and 15 unsuspicious eyes, who underwent both OCT angiography and FAG. The latter served as the gold standard for CNV diagnosis.

To determine the value of OCT angiography for monitoring the effect of intravitreal ranibizumab therapy, 9 CNV patients (9 eyes, of them 7 classic and 2 occult cases) going to receive their first injection were selected. The exam was performed the day before the injection and then at days 3, 10, 17, 24, and 31. Area measurements of the neovascular complex were taken with the same Z-offset.

Results and discussion

Three-dimensional imaging provided by OCT angiography enabled accurate localization of neovascular networks with respect to the RPE layer. Two groups were thus formed: group 1 — 43 eyes with neovascular growth beneath the RPE (CNV type 1, or occult) and group 2 — 29 eyes with most of their neovasculatures lying above the RPE (CNV type 2, or classic).

We have also described two possible configurations of the neovascular network: *tree-like* (notable for its large main trunk and dense branching) and *loop-like* (characterized by numerous twists and interlacements of the vessels). Moreover, all the lesions were classified as either well-, or ill-defined. The results obtained in the two study groups are summarized in **Table 1**.

As shown in **Table 1**, most of the patients in the occult CNV group (76.74%) had loop-like membranes ($p<0.05$). The lesions were well-defined in 55.8% of cases and ill-defined in 44.19%. Their mean area was 1.942±1.593 mm^2.

In the classic CNV group, the neovascular complex was clearly visible in 82.76% of eyes ($p<0.05$), loop-like and tree-like networks occurring with similar frequency (51.72% and 42.28% respectively). The mean area of classic CNV lesions was 1.178±0.945 mm^2.

Inter-group comparisons of OCT angiography results revealed that occult growth was most often associated with the formation of ill-defined loop-like membranes, while classic growth — with well-defined tree-like membranes ($p<0.05$).

Here we share some cases from our own experience.

Clinical case 1. Patient Z., a 63-year-old female with neovascular AMD in the right eye. Visual acuity (VA) OD = 1.0 (Golovin-Sivtsev chart). The woman presented complaints of seeing a blurry spot in front of her right eye for about two months. Her assessment included SD-OCT of the macula, fundus FAG, and OCT angiography. On examination, there was a yellowish parafoveal depos-

***Table 1*. OCT angiography presentation of the neovascular complex in patients with classic and occult CNV**

Parameter	CNV	
	Type 1 (occult)	Type 2 (classic)
Total number of eyes, abs — %±*m*	43 — 100±0	29 — 100±0
Tree-like configuration, abs — %±*m*	10 — 23.26±6.44	15 — 51.72±9.28**
Loop-like configuration, abs — %±*m*	33 — 76.74±6.44*,**	14 — 48.28±9.28
Well-defined, abs — %±*m*	24 — 55.81±7.57	24 — 82.76±7.01*,**
Ill-defined, abs — %±*m*	19 — 44.19±7.57**	5 — 17.24±7.01
Mean area of neovascularization, mm^2±*m*	1.942±1.593	1.178±0.945

Note. * — significant intra-group difference ($p<0.05$); ** — significant inter-group difference ($p<0.05$).

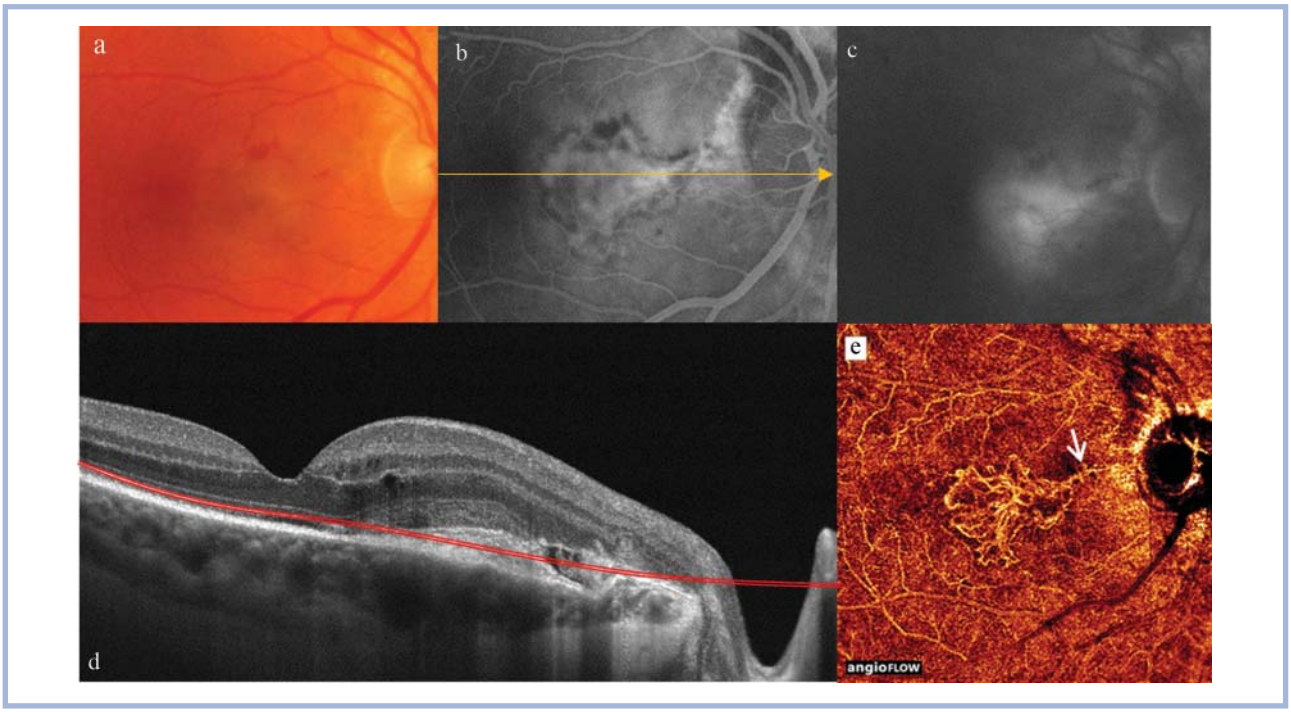

Fig. 1. **Clinical case 1, neovascular AMD (type 2, or classic, CNV)**

a — color photograph. A grey-yellow spot in the nasal para- and perifovea with few hemorrhages; b — early phase of FAG — a well-demarcated area of hyperfluorescence; c — late phase of FAG — leakage from a classic neovascular membrane; d — SD-OCT — a spindle-shaped hyperreflective lesion located at the level of the RPE in the para- and perifoveal area (along its nasal border the RPE is distorted and demonstrates abnormal concave curvature); numerous parafoveal intraretinal cavities; e — en face OCT angiography, 6x6 mm (segmentation boundaries are marked by the double red line in d) — an active vascular network above the RPE notable for dense branching and twisted loops. The supplying blood vessel (white arrow) starts at the optic disc margin.

it and few hemorrhages (**Fig. 1, a**). FAG was notable for a well-demarcated area of hyperfluorescence in its early phase and late leakage (**Fig. 1, b, c**). SD-OCT (**Fig. 1, d**) demonstrated a spindle-shaped hyperreflective lesion above the RPE. OCT angiography showed a loop-like neovasculature (**Fig. 1, e**) that spatially corresponded to the area of early hyperfluorescence by FAG and the spindle-shaped lesion by SD-OCT. Location of the segmented layer from the en face image is marked by the double red line in the B-scan (**Fig. 1, d**) showing that the vessels grow, indeed, above the RPE.

Clinical case 2. Patient S., 76-year old male with neovascular AMD in the right eye. Best corrected VA (BCVA) OD = 0.7. On presentation, the man complained of decreased vision in his right eye since 3 months. In the color fundus photograph (**Fig. 2, a**) one can see pigment redistribution within the fovea and nasal parafovea, partial atrophy of the RPE, and mild parafoveal elevation of the retina. During FAG (**Fig. 2, b, c**), early-phase diffuse juxta- and parafoveal hyperfluorescence and late-phase accumulation of the dye were noticed. SD-OCT (**Fig. 2, d**) showed a foveal neurosensory detachment as well as juxta- and parafoveal RPE detachment in the nasal retinal quadrant with heterogeneous hyperreflective content. OCT angiography (**Fig. 2, e**) enabled visualization of an intensively branched vascular network that resembled a tree and spatially corresponded to the area of early hyperfluorescence by FAG and the RPE detachment by SD-OCT. The level at which the en face image was obtained is marked by the double red line in the B-scan, thus, demonstrating that the neovasculature lies immediately within the sub-RPE space created by its serous detachment.

Our next step was to determine the value of OCT angiography in monitoring the effect of anti-VEGF therapy. To achieve this end, we studied dynamics of neovascular complexes in patients with different types of CNV under ranibizumab therapy. The results obtained are presented in **Table 2**.

As shown in **Table 2**, there were two classic cases, in which the area of neovascularization (0.16 and 0.73 mm^2 at baseline) had already decreased by day 3 after ranibizumab injection and regressed completely afterwards. However, small vessels were noticed above the RPE at days 24 and 17 respectively. In another classic case, the neovascular component had enlarged by day 3 and then slightly shrunk by day 10. Two patents with occult CNVs demonstrated a gradual decrease in the area of neovascularization during the first month after the injection starting from day 3.

Not only CNV areas, but also neovessels diameter, branching pattern and density could well be assessed with

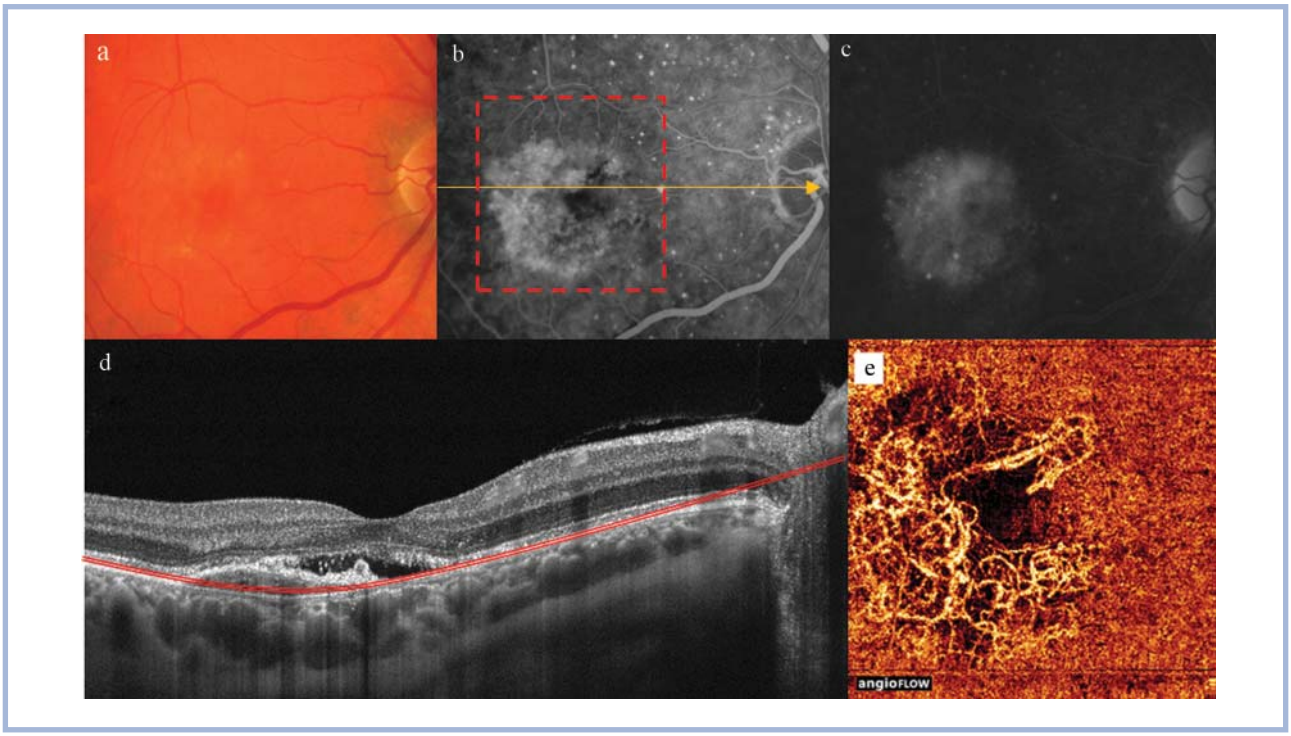

Fig. 2. **Clinical case 2, neovascular AMD (type 1, or occult, CNV)**

a — color photograph. Pigment redistribution within the fovea and nasal parafovea, mild parafoveal elevation of the retina, and dull macular reflex; b — early phase of FAG — a heterogeneous zone of hyperfluorescence; c — late phase of FAG — dye accumulation in the area of RPE detachment; d — SD-OCT — a foveal neurosensory detachment as well as juxta- and parafoveal RPE detachment in the nasal retinal quadrant with heterogeneous hyperreflective content; e — en face OCT angiography, 3x3 mm (the red dotted box in b and the double red line in d indicate the segmentation boundaries) — an active vascular network rich with loops lies within the sub-RPE space in the area of its detachment.

Table 2. **Area dynamics of neovascular complex in patients with classic and occult CNV receiving ranibizumab therapy**

Sex, age (years)	CNV		Neovascular complex area, mm²					
	type	shape	a day before the treatment	After the treatment				
				day 3	day 10	day 17	day 24	day 31
F, 60	classic	loop-like	0.16	0	0	0	0.03	0.05
M, 67	classic	tree-like	0.73	0.23	0	0.09	0.11	0.18
F, 70	classic	tree-like	2.68	2.27	2.13	1.94	1.27	1.19
F, 81	classic	loop-like	3.65	3.57	3.44	3.20	3.15	3.02
M, 76	classic	loop-like	0.42	1.73	1.65	1.65	1.54	1.50
F, 63	classic	loop-like	2.21	1.90	1.87	0.94	0.48	0.28
F, 67	occult	loop-like	9.53	9.31	9.34	9.22	9.01	8.95
F, 55	occult	loop-like	1.34	1.23	1.11	0.94	0.85	0.81

OCT angiography performed before and after intravitreal ranibizumab injection. Here are some examples to support that.

Clinical case 3. Patient M., a 67-year-old male, is being followed up due to neovascular AMD (classic CNV) in his left eye and has so far received one ranibizumab injection. Before the treatment his BCVA OS was 0.2. SD-OCT (**Fig. 3, a-d**) initially revealed a slit-like detachment of foveal RPE and a spindle-like hyperreflective lesion just above the epithelium. On follow-up SD-OCT scans the lesion showed a decrease in height, more significant in the nasal parafovea. OCT angiography (**Fig. 3, e-h**) evidenced an active vascular network with numerous branches sent nasal to the fovea (within the juxta- and parafoveal regions). Location of the segmented layer from the en face images demonstrates that the vessels grow, indeed, above the RPE. Three days after the injection, the density and diameter of neovessels decreased, small branches collapsed. No pathologic vascular activity is registered at day 13. At day 30 the patient's visual acuity OS is 0.2 +1.50sph => 0.4.

Clinical case 4. Patient M., an 88-year-old female, is being followed up due to neovascular AMD (mixed CNV) in her right eye. One ranibizumab injection has been ywt performed into the right eye. Before the treatment patient's BCVA OD was 0.09. SD-OCT at baseline

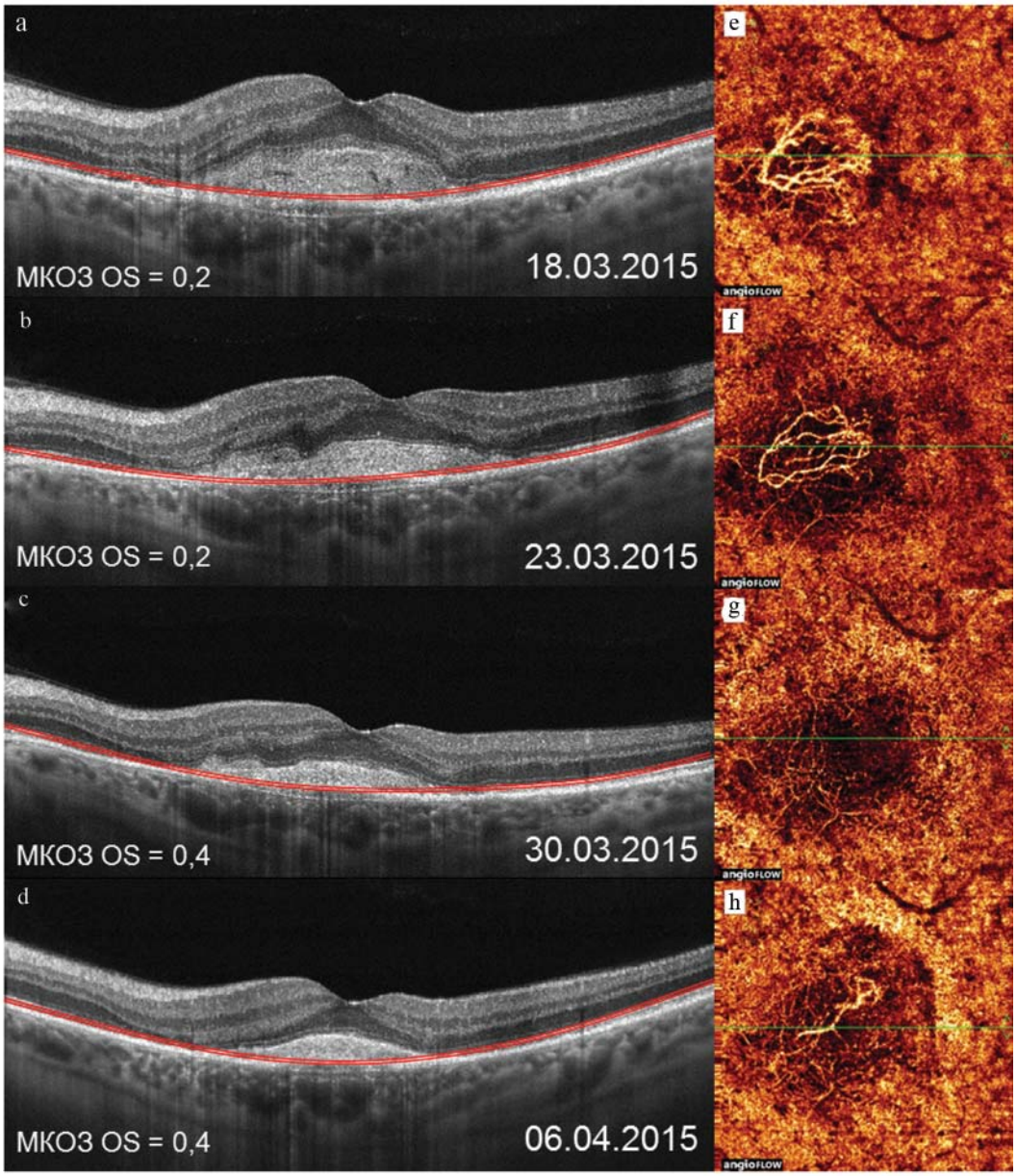

***Fig. 3*. Clinical case 3, neovascular AMD (type 2 CNV).**

SD-OCT results (B-scans a-d were obtained along the green line in e-h): a slit-like detachment of the foveal RPE and a spindle-like hyperreflective lesion just above; on follow-up scans (b-d) the lesion shows a gradual decrease in height. OCT angiography results, 3x3 mm (e-h, segmentation boundaries are marked by the double red line in a-d): a well-defined vascular network with numerous small branches located predominantly above the RPE (e); day 3 after intravitreal ranibizumab injection (IRI) — neovessels density and diameter has significantly decreased (f); day 10 after IRI — neovessels in the outer retina show no activity (g); day 17 after IRI — a long vessel with a loop-like ending is found right below the RPE (h).

(**Fig. 4, a**) revealed a slit-like detachment of foveal RPE and a parafoveal neurosensory detachment in the upper retinal quadrant. There was also a prominent hyperreflective lesion above the RPE. On follow-up SD-OCT scans (20 days after the injection) (**Fig. 4, b**) this lesion showed a decrease in height with subsequent decrease in central retinal thickness and complete reabsorption of subretinal fluid. OCT angiography (**Fig. 4 c, d**) demonstrated an active vascular network with one main trunk and numerous branches surrounded by small loops and, thus, resembling a tree. On a follow-up angiogram obtained at day 30 the neovasculature decreased in density, small vessels collapsed. Large branches on both sides of the RPE, however, remained active.

Having analyzed the results, we found that OCT angiography was positive in 33 out of 37 eyes with confirmed CNV, which means that the method's sensitivity is 89.2%. In a group of 15 patients with no signs of neovascularization on FAG, OCT angiography was positive in only 1 eye (6.7% of cases) and, thus, has specificity of 93.3%.

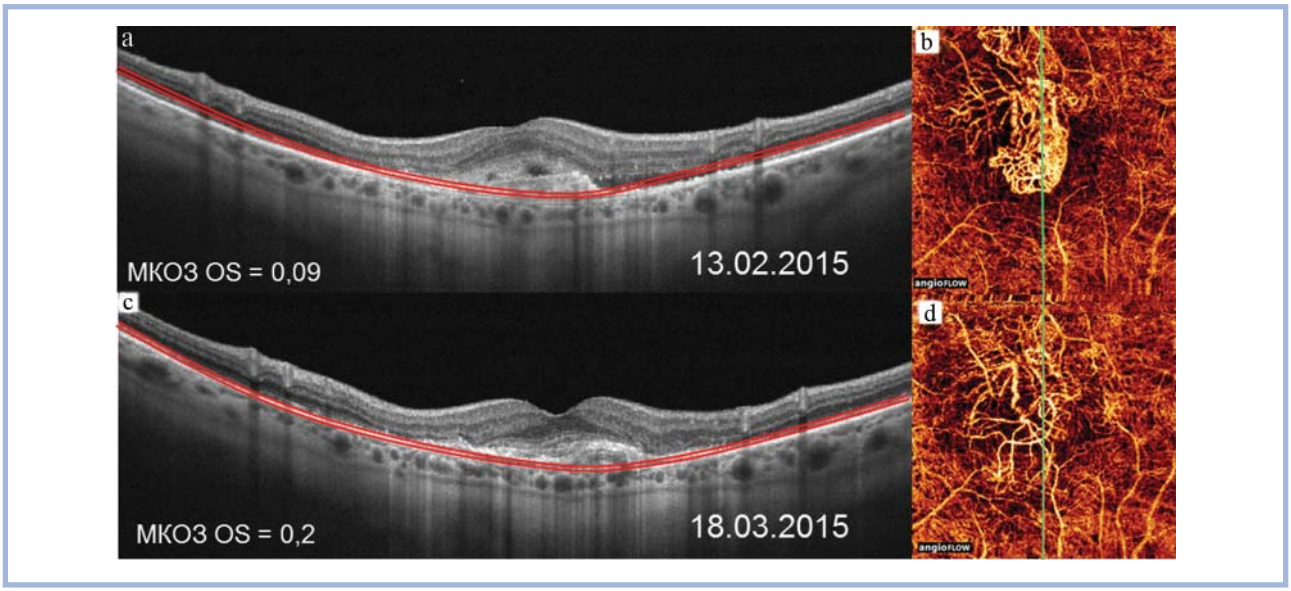

***Fig. 4*. Clinical case 4, neovascular AMD (mixed CNV).**

SD-OCT results (B-scans a and c were obtained along the green line in b and d): the spindle-like hyperreflective lesion above the RPE has decreased in height, the neurosensory detachment has fully resolved. OCT angiography results (b and d, segmentation boundaries are marked by the double red line in a and c): neovessels density and diameter has significantly decreased.

Introduction of spectral-domain optical coherence tomography led to a real breakthrough in terms of diagnosing many diseases, including age-related macular degeneration. This state-of-the-art diagnostic technology enabled morphological assessment of the retina and choroid, visualization of intra- and subretinal fluid (which is a sign of active CNV), and on-treatment monitoring of the damaged area and retinal thickness [17, 18]. It provides, however, very limited information on membrane configuration. SD-OCT also does not allow to measure the exact size of the neovascular complex since reflectivity of the latter is very similar to that of drusen, RPE, and choroid. [18]. Dye tracing methods fill the gap, but being invasive they may cause adverse effects and allergic reactions [12-14]. That is why OCT angiography, a non-invasive technique of fundus blood flow visualization that does not require an intravenous dye, became so widely used in clinical practice. The method is based on split-spectrum amplitude decorrelation angiography (SSADA) algorithm developed by D. Huang, Y. Jia et al. [15]. SSADA software analyzes amplitude differences between two laser beams that are emitted sequentially and then reflect from a particular point and/or scatter within the studied volume. The said difference will only be significant when the two beams are scanned across the interior of a blood vessel because scattering pattern of moving erythrocytes varies rapidly. The rest of the retina does not move and signal variations that may arise simply result from optical noise. Thus, decorrelation algorithm allows detection of blood flow/microcirculation. One can even say that in OCT angiography patient's blood flow serves as an endogenous contrast agent [15, 16]. To minimize the number of signal acquisitions without compromising the quality of the vascular map, the full OCT spectrum is split into several narrower spectral bands. Smaller bandwidths also reduce signal susceptibility to axial motion noise.

Since its patient's blood flow that serves as a contrast agent for OCT angiography, blood vessels can be displayed in a distinct color, thus, providing a clear idea of their structure and thickness as well as the area, configuration, and density of the network [15, 16]. 'Segmented layer' is an important term in OCT image analysis [16]. OCT angiogram can be segmented to display individual retinal and choroidal capillary beds, allowing three-dimensional appreciation of their blood flow [15, 16]. By scrolling through the en face scan one is able to evaluate changes in a particular layer of interest.

In our study, OCT angiography has proved reliable in distinguishing between the two types of CNV: occult and classic, new blood vessels growing beneath or above the RPE, respectively.

Moreover, the method has been shown capable of determining neovasculature configuration. Statistically significant differences in configuration between the two types of CNV have been found for the first time: occult membranes most often produce loops, while classic lesions are usually well-demarcated and resemble trees. The opportunity to measure the area of the neovascular complex enables studying its prognostic value for disease progression, under treatment in particular.

High safety of repeated exams suggests that OCT angiography can be used for monitoring treatment effects on neovascular networks [19-21]. Clinical cases reported here confirm that small neovessels become thinner and inactivate early after intravitreal ranibizumab injection. The effect is more pronounced in type 2 CNV (classic). Clinical implementation of our results and further studies

are needed to identify groups of patients at risk of developing tolerability or tachyphilaxis to anti-VEGF therapy.

High sensitivity and specificity of OCT angiography (89.2% and 93.3% respectively) that we have obtained agree with the results of De Carlo et al. [21], who reported 50% sensitivity and 91% specificity of the method in a sample of 30 participants with CNV.

Although being simple, visual, and informative, OCT angiography nevertheless has its limits. SSADA software detects erythrocytes passing through blood vessels but only those that move at a certain range of speeds [15, 16]. Therefore, if the blood flow is too slow or too fast, such vessels will not be displayed in the OCT angiogram. Moreover, scan quality is dependent on the transparency of the ocular media. Perhaps, this is why method sensitivity appears somewhat decreased exposing the need for further improvement.

Conclusion

1. OCT angiography has proved reliable in distinguishing between occult and classic CNVs in neovascular AMD patients. Classic membranes are usually well-defined tree-like lesions located predominantly above the RPE. On the contrary, occult growth takes place mostly beneath the RPE and produces loop-like membranes with ill-defined margins.

2. OCT angiography can be used to assess area dynamics of the neovascular complex under anti-VEGF therapy. It also gives idea of network configuration, branching pattern and vessels density.

3. With regard to CNV, occult or classic, OCT angiography has been shown to have 89.2% sensitivity and 93.3% specificity.

4. Non-invasiveness of OCT angiography and the high value of information provided determine its suitability for follow-up of AMD patients and evaluation of the effect of anti-VEGF therapy.

Author contributions:

Study conception and design — I.P., T.Sh.

Acquisition and handling of data — T.Sh., V.Sh., R.Sh.

Statistical analysis of data — T.Sh., T.Sh., R.Sh.

Drafting of manuscript — T.Sh., I.P., A.F.

Critical revision — I.P., T.Sh., V.Sh.

The authors declare no conflict of interest.

REFERENCES

1 Pascolini D, Mariotti S, Pokharel G et al. 2002 Global update of available data on visual impairment: a compilation of population-based prevalence studies. *Ophthalmic Epidemiology*. 2004;11(2):67-115.
doi:10.1076/opep.11.2.67.28158.

2 Klein R, Klein B, Linton K. Prevalence of Age-related Maculopathy. *Ophthalmology*. 1992;99(6):933-943.
doi:10.1016/s0161-6420(92)31871-8.

3 Ambati J, Ambati B, Yoo S, Ianchulev S, Adamis A. Age-Related Macular Degeneration: Etiology, Pathogenesis, and Therapeutic Strategies. *Survey of Ophthalmology*. 2003;48(3):257-293.
doi:10.1016/s0039-6257(03)00030-4.

4 Budzinskaya M. Age-related macular degeneration. Vestnik oftalmologii. 2014; 130(6): 56-61.

5 Silvester A. Age-related macular degeneration and its effect on quality of life. JRSM. 2009; 102(8): 310-310.
doi:10.1258/jrsm.2009.090137.

6 Hassell J. Impact of age related macular degeneration on quality of life. British Journal of Ophthalmology. 2006;90(5):593-596.
doi:10.1136/bjo.2005.086595.

7 Gass, J.D. Stereoscopic atlas of macular diseases. in: 4th ed. C.V. Mosby, St Louis, Missouri; 1997: 26–30

8 Yannuzzi L, Sorenson J, Spaide R, Lipson B. Idiopathic polypoidal choroidal vasculopathy (IPCV). Retina. 1990; 10(1): 1-8.
doi:10.1097/00006982-199001010-00001

9 Kokame G. Polypoidal Choroidal Vasculopathy — A Type I Polypoidal Subretinal Neovasculopathy. *TOOPHTJ*. 2013;7(1):82-84.
doi:10.2174/1874364101307010082.

10 Hartnett M, Weiter J, Garsd A, Jalkh A. Classification of retinal pigment epithelial detachments associated with drusen. *Graefe's Archive for Clinical and Experimental Ophthalmology*. 1992;230(1):11-19.
doi:10.1007/bf00166756.

11 Yannuzzi L. Retinal angiomatous proliferation in age-related macular degeneration. *Retina*. 2002;22(4):511-512.
doi:10.1097/00006982-200208000-00024

12 Complications from fluorescein angiography: a prospective study. *Clinical & Experimental Ophthalmology*. 2009;37(8):526-527.
doi:10.1111/j.1442-9071.2009.02158.x.

13 Lira R, Oliveira C, Marques M, Silva A, Pessoa C. Adverse reactions of fluorescein angiography: a prospective study. Arquivos Brasileiros de Oftalmologia. 2007;70(4):615-618.
doi:10.1590/s0004-27492007000400011.

14 Lipson B, Yannuzzi L. Complications of intravenous fluorescein injections. International Ophthalmology Clinics. 1989;29(3):200-205.
doi:10.1097/00004397-198902930-00011.

15 Jia Y, Tan O, Tokayer J et al. Split-spectrum amplitude-decorrelation angiography with optical coherence tomography. Opt Express. 2012;20(4):4710.
doi:10.1364/oe.20.004710.

16 Lumbroso B, Huang D, Jia Y, Fujimoto JA, Rispoli M. Clinical guide to Angio-OCT: Jjaypee; 2014.

17 Panova I.E., Prokopyeva M. Yu., Avdeeva O.N., Reznitskaya O.V. Clinical and instrumental monitoring in evaluation efficiency of different variants of neovascular age-related macular degeneration treatment. *Vestnik OGU*. 2011; 14: 292-294.

18 Giovannini A, Amato G, Mariotti C, Scassellati-Sforzolini B. OCT imaging of choroidal neovascularisation and its role in the determination of patients' eligibility for surgery. *British Journal of Ophthalmology*. 1999;83(4):438-442.
doi:10.1136/bjo.83.4.438.

19 Jia Y, Bailey S, Wilson D et al. Quantitative Optical Coherence Tomography Angiography of Choroidal Neovascularization in Age-Related Macular Degeneration. Ophthalmology. 2014;121(7):1435-1444.
doi:10.1016/j.ophtha.2014.01.034.

20 Marduel R (2015) Angio OCT, Dye Less Angiography, A New Approach of Age Related Macular Degeneration (ARMD). Adv Ophthalmol Vis Syst 2(2): 00034.
doi: 10.15406/aovs.2015.02.00034

21 de Carlo T, Bonini Filho M, Chin A et al. Spectral-Domain Optical Coherence Tomography Angiography of Choroidal Neovascularization. Ophthalmology. 2015.
doi:10.1016/j.ophtha.2015.01.029.